Transaction F: Nanotechnology
Vol. 17, No. 1, pp. 35–42
© Sharif University of Technology, June 2010

Invited Paper

SCIENTIA
IRANICA

Diffusion of Ionic Liquids into Elastomer/Carbon Nanotubes Composites and Tensile Mechanical Properties of Resulting Materials

B. Likozar[1]

Abstract. *In order to ensure better elastomer/functionalized Multi-Walled Carbon Nanotube (MWCNT) compatibility and to enhance the dispersion, a series of ionic liquids has been tested in regard to an improved interaction between elastomer and functionalized carbon nanotubes. We found that in the presence of especially one ionic liquid, namely, 1-butyl-1-methylpyrrolidinium tetrafluoroborate, for the hydrogenated nitrile elastomer, used as basic polymer, a 1.83 fold increase of elongation at break was achieved with only* ~ 7 *wt% ionic liquid loading. At this low concentration of ionic liquid the sample can be stretched up to 508% without mechanical failure. The use of this ionic liquid additionally results in high tensile strength (21.4 MPa) at low concentration* (< 7 *wt %) of ionic liquid. Energy-dispersive X-ray spectrometric scanning electron microscopy confirmed the homogeneous distribution of ionic liquids among nitrile elastomer chains by showing uniform signal belonging to fluorine in ionic liquid, when the diffusion process of ionic liquid into nanocomposites was long enough* (> 48 *h) during the ionic liquid absorption measurements. Transmission electron microscopic images confirmed the good dispersion of the MWCNT along with the exfoliated structure of the CNTs in the rubber matrix.*

Keywords: *Nanocomposites; Functionalized multi-walled carbon nanotubes; Ionic liquid; Elastomer; Polymer; Diffusion coefficient.*

INTRODUCTION

Tetrafluoroborate, hexafluorophosphate and *bis*(trifluoromethylsulfonyl)imide room temperature ionic liquids containing substituted imidazolium and pyrrolidinium cations, particularly 1-ethyl-3-methylimidazolium ($EMIm^+$), have received extensive attention over the past 30 years [1]. Angell et al. were one of the first to describe a new class of polymer electrolytes for secondary lithium batteries termed "polymer-in-salt" which are rubbery solid electrolytes possessing high ionic conductivities [2].

Recently, several studies were published investigating nitrile elastomer (NBR)/ionic liquid composites, because of the fact that NBR is generally resistant to oil, fuel and other chemicals. Its resilience makes NBR a useful material for several applications. Moreover, NBR's ability to withstand a wide range of temperatures makes it an ideal material especially for extreme applications. Among others, Marwanta et al. discovered improved ionic conductivity of NBR/ionic liquid composites [3], while Cho et al. developed a solid state actuator based on the poly(3,4-ethylenedioxythiophene) (PEDOT)/NBR/ionic liquid system [4]. The first group consequently revealed that NBR/$Li(CF_3SO_2)_2N$ composites with added imidazolium-type zwitterion posses even more improved ionic conductivity [5], while the second group discovered an electro-active conducting polymer actuator based on solid polymer electrolyte [6] consisting of NBR and room temperature ionic liquids and high ionic conductivity and mechanical strength of solid polymer electrolytes based on NBR/ionic liquid and its application to an electrochemical actuator [7]. The group of Cho et al., subsequently, more thoroughly examined various aspects of the developed solid state actuator based on the PEDOT/NBR/ionic liquid system, specifically, the effect of anion size of imidazolium ionic liquid [8] and the characteristics of

---

[1] *Faculty of Chemistry and Chemical Technology, University of Ljubljana, Aškerčeva cesta 5, 1000 Ljubljana, Slovenia. E-mail: blaz.likozar@fkkt.uni-lj.si*

Received 13 May 2010; accepted 30 August 2010

PEDOT/NBR/PEDOT solid actuator depending on the NBR polarity [9]. Parallel to this, they also examined a dry type conducting polymer actuator based on polypyrrole-NBR/ionic liquid system [10]. The mechanical properties of the mentioned composites, however, were not optimal, as these properties of the matrix material (NBR) compound were not considered in detail.

Elastomer/carbon nanotubes present themselves as an ideal solution to address this topic. However, studies of the subject are scarce. Silicone elastomer/carbon nanotubes/ionic liquid composites were used to produce a rubberlike stretchable matrix using elastic conductors [11]. A blend of styrene-butadiene rubber and polybutadiene rubber in combination with carbon nanotubes and ionic liquids was studied to determine coupling activity of ionic liquids between diene elastomers and multi-walled carbon nanotubes [12].

Therefore, in this study, the absorption and diffusion of different ionic liquids in hydrogenated NBR (HNBR) reinforced with hydroxyl-functionalized multi-walled carbon nanotubes (MWCNT-OH) was examined, HNBR exhibiting superior performance in comparison to NBR, whereas MWCNT-OH were utilized to provide excellent mechanical properties of the matrix material [13,14]. Tensile mechanical properties of the resulting materials were studied to determine the effect of the applied ionic liquids on functional properties.

EXPERIMENTAL

Hydrogenated nitrile rubber (HNBR) bulk was a gift from Erwin Mach Gummitechnik, GmbH. HNBR was used as received. HNBR with the acrylonitrile content of 34 wt% (confirmed by nitrogen analyzer) and the double bond content of 0.9 mol% (confirmed by infrared (IR) spectroscopy) was used in this study, because this is the best composition for its optimal physical properties, compromising strength and elasticity. The Mooney viscosity of HNBR was 70 at 100°C. 1-ethyl-3-methylimidazolium tetrafluoroborate ($EMImBF_4$) (98 mol%, colourless to orange liquid), 1-butyl-3-methylimidazolium tetrafluoroborate ($BMImBF_4$) (99 mol%, colourless to orange liquid), 1-butyl-1-methylpyrrolidinium tetrafluoroborate ($BMPyBF_4$) (99 mol%, colourless to yellowish solid), 1-ethyl-3-methylimidazolium hexafluorophosphate ($EMImPF_6$) (99 mol%, colourless to yellowish solid), 1-butyl-3-methylimidazolium hexafluorophosphate ($BMImPF_6$) (99 mol%, colourless to orange liquid), 1-butyl-1-methylpyrrolidinium hexafluorophosphate ($BMPyPF_6$) (99 mol%, colourless to yellowish solid), 1-ethyl-3-methylimidazolium *bis*(trifluoromethylsulfonyl)imide (EMImTFSI) (99 mol%, colourless to orange liquid), 1-butyl-3-methylimidazolium *bis*(trifluoromethylsulfonyl)imide (BMImTFSI) (99 mol%, colourless to orange liquid), and 1-butyl-1-methylpyrrolidinium *bis*(trifluoromethylsulfonyl)imide (BMPyTFSI) (99 mol%, colourless to orange liquid), purchased from IoLiTec Ionic Liquids Technologies, GmbH, were used as received. The structure of the ionic liquids was confirmed by Nuclear Magnetic Resonance (NMR) and IR spectroscopy, and is presented in Figure 1. The mentioned ionic liquids were used in this study, because they should provide good electrical properties.

Samples with the thickness of 1 mm were obtained by pressing the compounds, reinforced with mixed-into-rubber hydroxy-functionalized multi-walled carbon nanotubes (MWCNT-OH) (purchased from Cheap Tubes, Inc., 90 wt% purity, confirmed by Raman spectroscopy), between steel plates at 180°C for 4.5 min to obtain cross-linked structure. Just after HNBR had cooled down to the room temperature (1 day) to prevent later solvent evaporation due to increased temperature, following vulcanization, composites containing the ionic liquids were prepared, so that HNBR samples were immersed into the excessive amount of the ionic liquids (HNBR/ionic liquid weight ratios of at least 1/10) in borosilicate glass tubes for different times (presented in Table 1) so that the ionic liquids diffused into the samples, while the ionic liquids were dissolved in chloroform (purchased from J.T.Baker, Inc., 99.5 wt% purity) in the weight ratio of 1/1, and stirred to obtain homogeneous solutions. Chloroform was

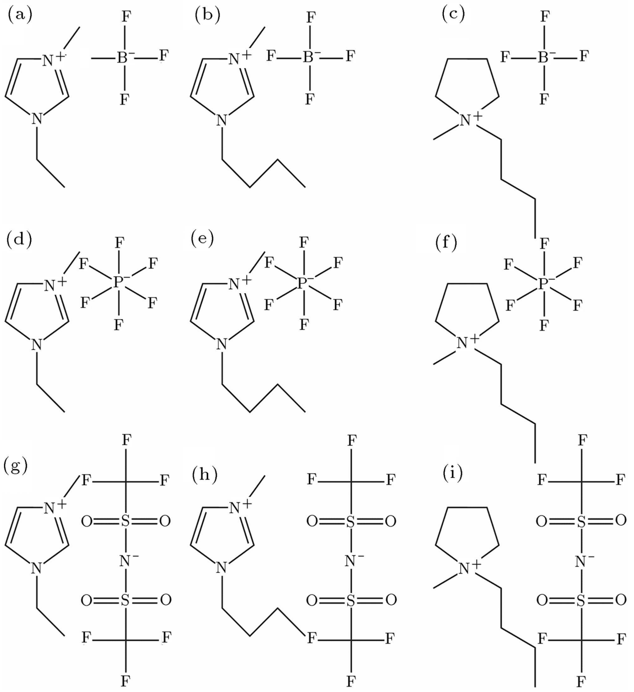

Figure 1. Ionic liquids applied to HNBR/MWCNT-OH composites: (a) $EMImBF_4$; (b) $BMImBF_4$; (c) $BMPyBF_4$; (d) $EMImPF_6$; (e) $BMImPF_6$; (f) $BMPyPF_6$; (g) EMImTFSI; (h) BMImTFSI; (i) BMPyTFSI.

Table 1. Immersion times of HNBR/MWCNT-OH composites in different ionic liquids.

Ionic Liquid	**Time (h)**			
$EMImBF_4$	/	/	/	48
$BMImBF_4$	/	/	/	48
$BMPyBF_4$	6	12	24	48
$EMImPF_6$	/	/	/	48
$BMImPF_6$	/	/	/	48
$BMPyPF_6$	/	/	/	48
EMImTFSI	6	12	24	48
BMImTFSI	/	/	/	48
BMPyTFSI	6	12	24	48

used in this study, because it enhanced the diffusion of the ionic liquids into the samples and dissolved the ionic liquids, which were in the solid state at the room temperature. After solvent removal, the samples were dried at the room temperature for 5 days to obtain solvent-free composites. The samples' dimensions increased, depending on the uptake of an ionic liquid and the solvent, and then decreased after the solvent removal to between 100 and 110% of the original values.

The tensile test (mechanical properties - global sample stress and strain measurement) of vulcanized HNBR/MWCNT-OH/ionic liquid composite sheets' dumbbell samples with the dimensions of $1\times4\times80$ mm was performed using MTS Polymer Test System (MTS Systems Corporation, Inc., USA) testing machine at the room temperature and in the displacement range from 0 to 100 mm. The maximum load was not set and elongation rate was 500 mm/min. The samples were put between two steel fixtures with 2 cm space in between.

The morphology of vulcanized HNBR/MWCNT-OH/ionic liquid composite sheet samples with the dimensions of $1\times4\times4$ mm was observed using scanning electron microscopy (SEM) (cut samples' surfaces) with Zeiss DSM 962 (Carl Zeiss, AG, Germany) microscope at the room temperature and in vacuum, using the acceleration voltage of 15 kV. INCAPentaFETx3 energy-dispersive X-ray spectrometer (EDX) (Oxford Instruments, PLC, UK), attached to SEM, was used to determine the chemical composition of the samples. The samples were fixed onto sample holder using conductive carbon cement, sputtered with carbon, and painted on the side with silver paste. Transmission electron microscopy (TEM) observations were performed with FEI Tecnai 12 (USA) microscope equipped with the embedded CCD camera at the acceleration voltage of 120 kV (the room temperature- and the cryo-cut samples with the thickness of 85 nm and 120-150 nm, respectively).

RESULTS AND DISCUSSION

HNBR/MWCNT-OH composites were subjected to ionic liquids, which diffused in the latter. Uptake was monitored at different times as presented in Table 1. Figure 2 shows the experimentally measured average ionic liquid weight fraction in composites as a function of time for $BMPyBF_4$, EMImTFSI and BMPyTFSI. It may be observed that these ionic liquids exhibit fast initial diffusion when the bulk of HNBR/MWCNT-OH may still be considered semi-infinite medium that is without any ionic liquid present, whereas after 24 h a clear equilibration process is exhibited, ionic liquids in HNBR/MWCNT-OH composites steadily reaching equilibrium absorption values alongside with diffusion rate decrease. Due to this conventional Fickean behavior, the diffusion was described using Fick's second law:

$$\frac{\partial C_{IL}}{\partial t} = D_{IL,C}\frac{\partial^2 C_{IL}}{\partial x^2}, \tag{1}$$

With accompanying initial and boundary conditions:

$$\begin{aligned} &C_{IL} = 0, && t = 0, \quad x \geq 0, \\ &C_{IL} = C_{IL,EQ}, && t > 0, \quad x = L, \\ &\frac{\partial C_{IL}}{\partial x} = 0, && t > 0, \quad x = 0. \end{aligned} \tag{2}$$

In Equations 1 and 2, C_{IL} (wt %) represents the concentration of ionic liquid at position x and at time t, $x = L$ corresponding to composite surface and $x = 0$ corresponding to composite middle (approximately 1 mm). It has to be noted that the

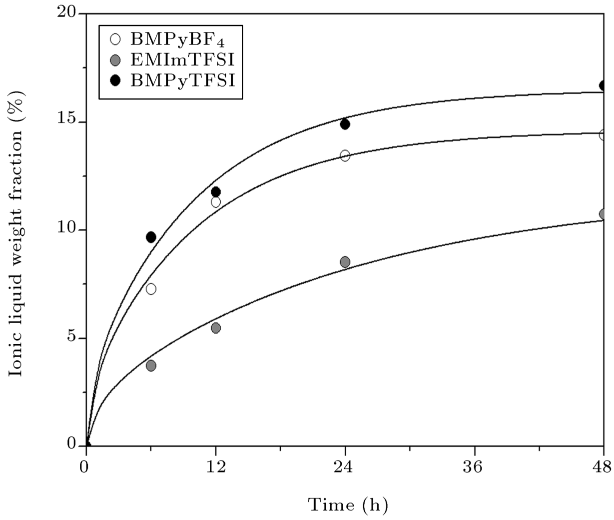

Figure 2. Average ionic liquid weight fractions in HNBR/MWCNT-OH composites obtained from experiment (symbols) and model (lines) as a function of immersion time.

HNBR/MWCNT-OH composite specimens had slab geometry and consequently the diffusion proceeded in x, as well as y and z directions. The latter two characteristic dimensions, however, were relatively larger than L, thus the concentration gradients were much lower and subsequently y and z diffusion fluxes could have been neglected. $D_{IL,C}$ is the diffusion coefficient of ionic liquid into HNBR/MWCNT-OH composite, while $C_{IL,EQ}$ represents the equilibrium uptake of ionic liquid. The solution of Equation 1, using the initial/boundary conditions of Equation 2, may be expressed by the following relationship:

$$\begin{aligned}C_{IL} =& C_{IL,EQ}\left(1-\frac{2}{\pi}\sum_{n=0}^{\infty}\frac{(-1)^n}{n+1/2}\right.\\ &\exp\left(-\pi^2(n+1/2)^2\frac{D_{IL,C}t}{L^2}\right)\\ &\left.\cos\left(\pi(n+1/2)\left(\frac{x}{L}\right)\right)\right). \qquad (3)\end{aligned}$$

As the average weight fraction was determined experimentally, Equation 3 had to be averaged along the diffusion direction axis x as well, specifically:

$$\langle C_{IL}\rangle = \frac{1}{L}\int_0^L C_{IL}dx. \qquad (4)$$

This resulted in the volume-averaged weight fraction $< C_{IL} >$ as expressed by the following equation:

$$\begin{aligned}\langle C_{IL}\rangle =& C_{IL,EQ}\left(1-\frac{2}{\pi^2}\sum_{n=0}^{\infty}\frac{1}{(n+1/2)^2}\right.\\ &\left.\exp\left(-\pi^2(n+1/2)^2\frac{D_{IL,C}t}{L^2}\right)\right). \qquad (5)\end{aligned}$$

This equation was fitted to the experimental data presented in Figure 2. The first 100 terms of the infinite series in Equation 5 proved to provide a good enough level of accuracy. $D_{IL,C}$ and $C_{IL,EQ}$ were varied as fitting parameters initially the latter assuming approximated values of 10^{-9} m^2/s and $< C_{IL} >$ at 48 h of immersion, respectively. These two parameters were regressed minimizing the sum of squares of differences between experimentally determined and model predicted $< C_{IL} >$ values. Model predictions of $< C_{IL} >$ for BMPyBF$_4$, EMImTFSI and BMPyTFSI are presented in Figure 2 as well, and it may be observed that the correspondence is quite good. The determined $C_{IL,EQ}$ were 14.6, 11.8, and 16.5 wt % for BMPyBF$_4$, EMImTFSI, and BMPyTFSI, respectively, and these values agree quite well with experimentally determined average weight fractions of ionic liquids at 48 h immersion time presented in Table 2, that is 14.4, 11.4, and 16.8 wt % for BMPyBF$_4$, EMImTFSI, and BMPyTFSI, respectively. The estimated diffusion coefficients were 1.10×10^{-11} m^2/s, 4.61×10^{-12} m^2/s, and 1.11×10^{-11} m^2/s for BMPyBF$_4$, EMImTFSI, and BMPyTFSI, respectively. These values would imply the cation predominantly determines the diffusion behavior, the diffusion coefficients of BMPyBF$_4$ and BMPyTFSI being almost the same. An interesting fact is that the diffusion coefficient of EMImTFSI is 2.4-fold lower than the other two mentioned, even though EMImTFSI itself is smaller in size, as ordinarily smaller component would be expected to diffuse faster in a given medium. This may be explained through the polarity of ionic liquids, specifically, BMPyBF$_4$ and BMPyTFSI, that is BMPy$^+$ cation has butyl group bonded to ionic liquid, which apparently increases the compatibility with the non-polar segments of HNBR chains and overall enhances mass transfer as compared to ethyl group bonded in EMIm$^+$ cation. This will also be discussed in the continuation of this paper. It is also interesting that anion, even as large as TFSI$^-$, does not have a noticeable impact on the diffusion rate. Quite the opposite, the equilibrium uptake seems to be higher for BMPyTFSI as for BMPyBF$_4$, even though TFSI$^-$ anion is substantially larger than BF$_4^-$. This once again may be explained through compatibility; TFSI$^-$ anion being in this case more compatible with the polar acrylonitrile segments of HNBR chains.

Table 2. Uptake of different ionic liquids by HNBR/MWCNT-OH composites at the immersion time of 48 h.

Ionic Liquid	**Uptake (wt %)**
EMImBF$_4$	1.8
BMImBF$_4$	2.6
BMPyBF$_4$	14.4
EMImPF$_6$	4.6
BMImPF$_6$	4.7
BMPyPF$_6$	6.4
EMImTFSI	11.4
BMImTFSI	17.6
BMPyTFSI	16.8

As only volume-averaged weight fractions of ionic liquids are presented in Figure 2, position- and time-dependency of BMPyBF$_4$ weight fraction is demonstrated in Figure 3. As shown the weight fraction is initially zero throughout the HNBR/MWCNT-OH composite, it then step-wise increases to $C_{IL,EQ}$ at the composite surface ($x/L = 1$), whereas it decreases more gradually in the bulk material, especially in the composite center ($x/L = 0$). Worth noticing is the fact that after 48 h, the distribution of C_{IL} is relatively uniform and close to $C_{IL,EQ}$, which could have already been expected from volume-averaged weight fractions in Figure 2. This is quite positive observation

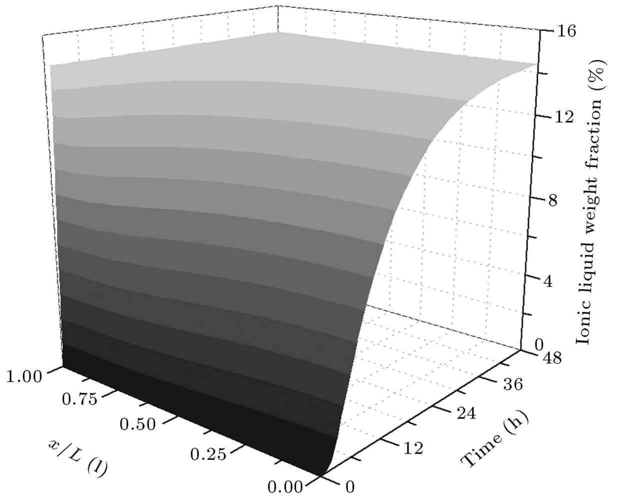

Figure 3. Model predicted $BMPyBF_4$ weight fractions in HNBR/MWCNT-OH composites as a function of immersion time and position in composites ($x/L = 1$ for the composite surface; $x/L = 0$ for the composite center).

as a homogeneous HNBR/MWCNT-OH composite is expected to be obtained within 48 h, at least as far as ionic liquid distribution is concerned. A question was, whether this could be validated experimentally and if the same applies for the distribution MWCNT-OH.

Therefore transmission and scanning electron microscopy of the cross-section of composites was examined and is presented in Figure 4. Carbon nanotubes, obtained by catalytic chemical vapor deposition, were used as received. When the carbon nanotubes were directly mixed with HNBR in a mixer, their dispersion was good as evidenced by the absence of any large MWCNT aggregates and any large isolated amount of rubber matrix without carbon nanotubes as filler in Figure 4a. That is, melt compounding gives a fine and uniform dispersion of carbon nanotubes in HNBR, as shown in Figure 4a. It can be seen that the cross-section dimensions of the dispersed carbon nanotubes' aggregates are quite small (tens of nanometers) with a few tens of micrometers-scale length. This causes some difficulties in clearly observing the diameter and the length of nanotubes with TEM at once, especially in distinguishing the length of individual carbon tubes. The interface between the carbon tubes and HNBR is greatly improved by the functionalization of nanotubes in the case of HNBR/MWCNT-OH nanocomposites. This definitely enhanced the tensile strength of carbon nanotubes composite. The dispersion quality of carbon nanotubes in the mentioned rubber matrix is truly quite satisfactory. Moreover, Figure 4b shows the detected ionic liquid homogeneity by observing fluorine signal of the latter utilizing SEM-EDX analysis of HNBR/MWCNT-OH/BMPyTFSI composite after 48 h immersion time. This validates the calculated uniformity of ionic liquid within the composite bulk.

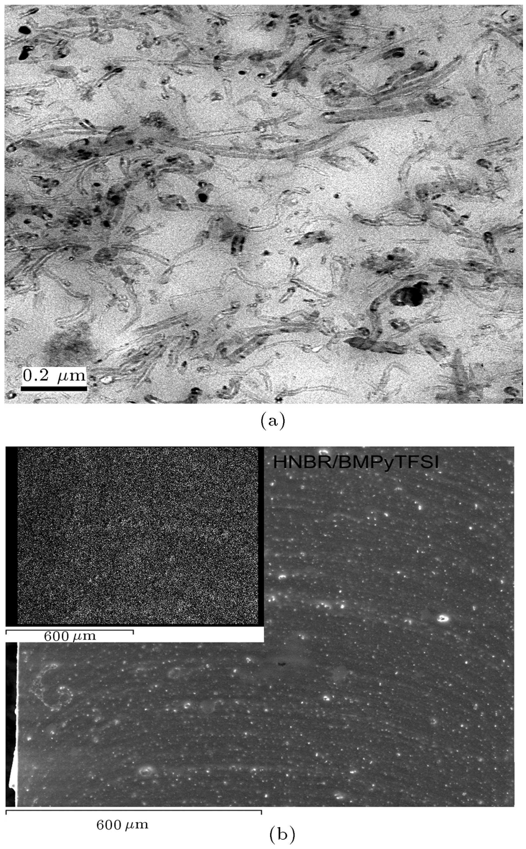

Figure 4. TEM microgram (a) and SEM combined with fluorine SEM-EDX micrograms (b) for HNBR/MWCNT-OH/BMPyTFSI composites.

Analogous observations were obtained for all composites and HNBR/MWCNT-OH/BMPyTFSI composite is presented due to a relatively high ionic liquid uptake and consequently strong fluorine signal.

Uptake of different ionic liquids by HNBR/MWCNT-OH composites at the immersion time of 48 h is presented in Table 2. The findings observed for $BMPyBF_4$, EMImTFSI and BMPyTFSI should generally be valid for other ionic liquids as well. This is indeed the case as equilibrium ionic liquid uptake more or less increased with decreasing cation polarity, the latter decreasing $EMIm^+ < BMIm^+ < BMPy^+$. Analogously as before the anion polarity determined uptake as well, nevertheless, not as much regularly as for cations. Subsequently, the uptake of all ionic liquids containing $TFSI^-$ is much higher than the comparable ones containing BF_4^- and PF_6^- and may in turn also be explained through compatibility with nitrile groups in polar HNBR segments. This led us to believe that the equilibrium uptake of an ionic liquid of the types which were utilized in this study may be in some way correlated to molecular mass, either of the ionic liquid or the positive/negative ion, constituting the ionic liquid. Therefore, several relatively simple expressions were tested to correlate either molecular mass with equilibrium uptake and power-law dependence proved to give the best results in terms of agreement followed only by high-degree polynomials, which nonetheless require more parameters for a correlation. Therefore, a power-law was chosen as the best option considering both number of adaptable parameters and correlation agreement. The correlated experimental data and the correlation itself are presented in Figure 5. Agreement is indeed good, whereas the exponent value is normally negative if the components of the same polarity, yet different molecular mass, are considered. In our case the polarity was intrinsically connected to molecular mass and it has to be noted that although the agreement was good in our case, this may not necessarily apply to other classes of ionic liquids. The ionic liquids applied in this study, however, are one of the most widespread ones and thus the practical value of the correlation still stands.

The mechanical properties of HNBR/MWCNT-OH composites immersed in ionic liquids for different times were tested in tensile mode in order to determine functional properties of the composites. Characteristic properties are presented in Figures 6 and 7 and Table 3. As evident from the mentioned figures and table tailor-made composite properties may be obtained with elongation at break as high as 508%, tensile strength as high as 24.3 MPa, and elastic modulus ranging to 16.6 MPa. These values are superb. However, they may not be obtained simultaneously but certain compromises have to be agreed on. From Figure 6b it may be seen that HNBR/MWCNT-OH composites with BMPyBF$_4$, EMImTFSI and BMPyTFSI all exhibit a minimum of tensile strength at 24, 12, and 6 h of immersion time, respectively, for the last two ionic liquids corresponding to minima in elongation at break. These two ionic liquids also exhibit elastic modulus minima, however, not at the same ionic liquid uptake, but at lower (EMImTFSI, immersion time 6 h) or higher (BMPyTFSI, immersion time 24 h) one, as demonstrated in Figure 7. All these properties were visibly improving with immersion time increasing from 12 h on for EMImTFSI and from 24 h on for BMPyTFSI. The same did not apply for BMPyBF$_4$ composites as the latter exhibit a maximum in elongation at break corresponding to minimum elastic modulus at 6 h immersion time, whereas the minimum in tensile strength ensued at 24 h immersion time. This particular type of behavior may be attributed to special interactions among ionic liquid and carbon nanotube domains [12], which result both in distinct relaxation processes of various domains as well as degradation processes and defect accumulation being specific to a

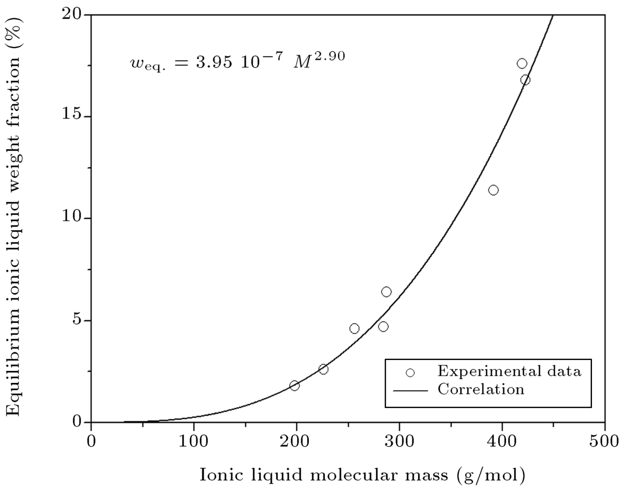

Figure 5. Equilibrium ionic liquid weight fractions in HNBR/MWCNT-OH composites obtained from experiment (symbols) and correlation (lines) as a function of ionic liquid molecular mass.

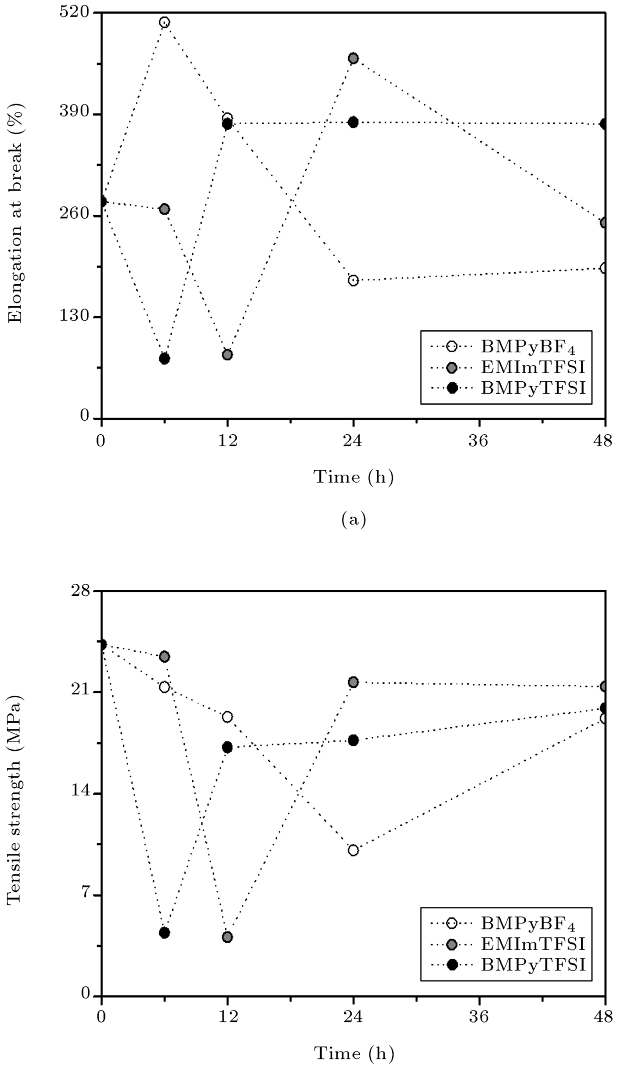

(a)

(b)

Figure 6. Elongation at break and tensile strength of HNBR/MWCNT-OH/ionic liquid composites as a function of immersion time.

Table 3. Tensile mechanical properties of HNBR/MWCNT-OH/ionic liquid composites.

Ionic Liquid	Tensile Strength (MPa)	Elongation at Break (%)	Elastic Modulus (MPa)
$EMImBF_4$	23.4	216	16.6
$BMImBF_4$	23.4	223	16.1
$BMPyBF_4$	19.2	193	14.2
$EMImPF_6$	23.3	227	16.2
$BMImPF_6$	23.4	280	15.6
$BMPyPF_6$	19.1	185	15.3
EMImTFSI	21.4	251	13.0
BMImTFSI	17.8	250	12.0
BMPyTFSI	19.9	378	10.6

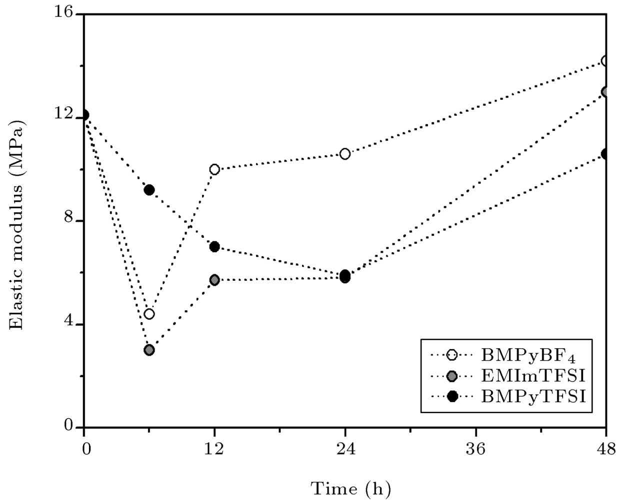

Figure 7. Elastic modulus of HNBR/MWCNT-OH/ionic liquid composites as a function of immersion time.

particular HNBR/MWCNT-OH/ionic liquid composition. From Table 3, the most promising composites are definitely the ones containing either $BMImPF_6$ or BMPyTFSI; the first one having second best elongation at break, the best tensile strength and relatively high elastic modulus among composites immersed in ionic liquids for 48 h. The second with BMPyTFSI has lower elastic modulus and slightly lower tensile strength as well, nevertheless has by far the greatest elongation at break. For all the applied ionic liquids electrical and ionic conductivity was studied extensively [3-10], so this aspect of functional properties is not questionable. Other functional properties, e.g. thermal and wear properties, were demonstrated to be excellent as well [13,14]. Not as many correlations may be made between ionic liquid structure and mechanical properties as tensile strength and elongation at break in Table 3 do not seem to exhibit a particular trend as far as cation and anion type are concerned. Elastic modulus, nonetheless seems to decrease with decreasing cation polarity, which may be explained by the fact that decreasing polarity causes higher equilibrium absorption of ionic liquid (as discussed before) which in turn results in plasticizing effect of the ionic liquid; the latter softening the reinforced matrix. All in all, the choice of particular ionic liquid and nanocomposite composition resulting from the choice of suitable immersion time are strongly dependent on the final application in question, whether there should be a demand for a stiff, rigid material intended for low deformations or, on the other hand, a material which should withstand large strains, but is not necessarily as stiff as the one mentioned before.

CONCLUSIONS

Functionalized multi-walled carbon nanotubes along with an ionic liquid 1-butyl-1-methylpyrrolidinium tetrafluoroborate ($BMPyBF_4$) provide a strong level of reinforcement to an HNBR rubber matrix. The chemical coupling between carbon nanotubes and rubber chains by $BMPyBF_4$ is evidenced by mechanical properties such as elongation at break and elastic modulus. It was found that $BMPyBF_4$ probably plays a major role in enhancing the level of dispersion, and thus superior mechanical properties, such as elongation at break and tensile strength, have been achieved. The morphology of the nanocomposite, especially the CNT dispersion was examined, whereas the ionic liquid homogeneity was detected by observing fluorine signal of the latter utilizing SEM-EDX.

ACKNOWLEDGMENTS

This work was supported by the Austrian Research Promotion Agency Structural Programme (K*plus* - Competence Centers Programme). The author also acknowledges the support of Dr. Zoltan Major.

REFERENCES

1. Fuller, J., Breda, A.C. and Carlin, R.T. "Ionic liquid-polymer gel electrolytes", *J. Elektrochem. Soc.*, **144**(4), pp. L67-L69 (1997).
2. Angell, C.A., Liu, C. and Sanchez, E. "Rubbery solid electrolytes with dominant cationic transport and high ambient conductivity", *Nature*, **362**(6416), pp. 137-139 (1993).
3. Marwanta, E., Mizumo, T., Nakamura, N. and Ohno, H. "Improved ionic conductivity of nitrile rubber/ionic liquid composites", *Polymer*, **46**(11), pp. 3795-3800 (2005).
4. Cho, M.S., Seo, H.J., Choi, H.R., Koo, J.C., Song, K.G. and Lee, Y. "A solid state actuator based on the PEDOT/NBR system", *Sensor. Actuat. B-Chem.*, **119**(2), pp. 621-624 (2006).
5. Marwanta, E., Mizumo, T. and Ohno, H. "Improved ionic conductivity of nitrile rubber//Li($CF_3SO_2)_2N$ composites by adding imidazolium-type zwitterion", *Solid State Ionics*, **178**(3-4), pp. 227-232 (2007).
6. Cho, M.S., Seo, H.J., Nam, J., Choi, H.R., Koo, J.C. and Lee, Y. "An electroactive conducting polymer actuator based on NBR/RTIL solid polymer electrolyte", *Smart Mater. Struct.*, **16**(2), pp. S237-S242 (2007).
7. Cho, M.S., Seo, H.J., Nam, J., Choi, H.R., Koo, J.C. and Lee, Y. "High ionic conductivity and mechanical strength of solid polymer electrolytes based on NBR/ionic liquid and its application to an electrochemical actuator", *Sensor. Actuat. B-Chem.*, **128**(1), pp. 70-74 (2007).
8. Cho, M.S., Seo, H.J., Nam, J., Lee, Y. and Son, Y.K. "A solid state actuator based on the PEDOT/NBR system: effect of anion size of imidazolium ionic liquid", *Mol. Cryst. Liq. Cryst.*, **464**, pp. 51-56 (2007).
9. Cho, M.S., Seo, H.J., Nam, J., Lee, Y., Choi, H.R., Koo, J.C. and Son, Y.K. "Characteristics of PEDOT/NBR/PEDOT solid actuator depending on the NBR polarity", *Mol. Cryst. Liq. Cryst.*, **472**, pp. 289-296 (2007).
10. Cho, M.S., Nam, J., Lee, Y., Choi, H.R. and Koo, J.C. "Dry type conducting polymer actuator based on polypyrrole-NBR/ionic liquid system", *Mol. Cryst. Liq. Cryst.*, **444**, pp. 241-246 (2006).
11. Sekitani, T., Noguchi, Y., Hata, K., Fukushima, T., Aida, T. and Someya, T. "A rubberlike stretchable matrix using elastic conductors", *Science*, **321**(5895), pp. 1468-1472 (2008).
12. Das, A., Stöckrlhuber, K.W., Jurk, R., Fritzche, J., Klüppel, M. and Heinrich, G. "Coupling activity of ionic liquids between diene elastomers and multiwalled carbon nanotubes", *Carbon*, **47**(14), pp. 3313-3321 (2009).
13. Likozar, B. "Modeling of chemical kinetics of elastomer/hydroxyl- and carboxyl-functionalized multi-walled carbon nanotubes (MWCNT) nanocomposites' cross-linking", *Polym. Eng. Sci.* (In press).
14. Likozar, B. and Major, Z. "Morphology, mechanical, structural, thermodynamic, and functional properties of (hydrogenated) nitrile rubber/(un)functionalized multi-walled carbon nanotubes composites prepared by melt compounding: The effect of acrylonitrile content and hydrogenation", *Appl. Surf. Sci.*, **257**(2), pp. 565-573 (2009).

BIOGRAPHY

Blaû Likozar (born in Kranj, Slovenia in 1981) earned his Ph.D. in Chemical Engineering at the Faculty of Chemistry and Chemical Technology of the University of Ljubljana (Slovenia). After his Ph.D. in 2008 and the postdoctoral research at the University of Leoben (Austria), he became an assistant professor of chemical engineering at the Chair of Chemical, Biochemical and Environmental Engineering. His research is focused on synthesis and characterization of elastomer nanocomposites containing carbon nanotubes and the production of biodiesel using microalgae.